Published in final edited form as:
J Proteome Res. 2008 August ; 7(8): 3543–3555. doi:10.1021/pr800286z.

Imaging Mass Spectrometry of Intact Proteins from Alcohol-Preserved Tissue Specimens: Bypassing Formalin Fixation

Pierre Chaurand[*,†], **Joey C. Latham**[†], **Kirk B. Lane**[‡], **James A. Mobley**[§], **Vasiliy V. Polosukhin**[‡], **Pamela S. Wirth**[||], **Lillian B. Nanney**[||], and **Richard M. Caprioli**[†]
Mass Spectrometry Research Center and Department of Biochemistry, Vanderbilt University School of Medicine, Nashville, Tennessee 37232-8575, Department of Allergy/Pulmonary and Critical Care Division, Vanderbilt University School of Medicine, Nashville, Tennessee 37232-2650, Department of Surgery, Division of Urology, University of Alabama in Birmingham, Birmingham, Alabama 35294, and Department of Plastic Surgery and the Immunohistochemistry Core Laboratory, Vanderbilt University School of Medicine, Nashville, Tennessee 37232-2631

Abstract

Imaging mass spectrometry is becoming a key technology for the investigation of the molecular content of biological tissue sections in direct correlation with the underlying histology. Much of our work has been done with fresh-frozen tissue sections that has undergone minimal protein degradation between the time a tissue biopsy is sampled and the time it is snap-frozen so that no preserving or fixing agents need to be added to the frozen biopsy. However, in many sampling environments, immediate flash freezing may not be possible and so we have explored the use of ethanol-preserved, paraffin-embedded tissue specimens for proteomic analyses. Solvent-only preserved tissue specimens provide long-term preservation at room temperature, generation of high quality histological sections and little if any chemical alteration of the proteins. Using mouse organs, several key steps involved in the tissue dehydration process have been investigated to assess the potential of such preserved specimens for profiling and imaging mass spectrometry investigations.

Keywords

Ethanol preserved; Tissue; Proteins; Imaging mass spectrometry; MALDI

Introduction

In recent years, matrix-assisted laser desorption-ionization imaging mass spectrometry (MALDI IMS) has been used to measure proteins in tissue specimens through the direct analysis of thin sections. This technology is advantageous because of its capability of high throughput and ability to provide information on the localization and relative abundance of multiple molecules in a sample. Recent applications of this technology clearly show native

[*]To whom correspondence should be addressed. Pierre Chaurand, Mass Spectrometry Research Center, 9160 MRB III, Vanderbilt University, Nashville TN, 37232-8575, Tel: (+1) 615 343 8369. Fax: (+1) 615 343 8372. pierre.chaurand@vanderbilt.edu.
[†]Mass Spectrometry Research Center and Department of Biochemistry, Vanderbilt University School of Medicine.
[‡]Department of Allergy/Pulmonary and Critical Care Division, Vanderbilt University School of Medicine.
[§]Department of Surgery, University of Alabama in Birmingham.
[||]Department of Plastic Surgery and the Immunohistochemistry Core Laboratory, Vanderbilt University School of Medicine.

Supporting Information Available: Tables listing proteins identified in the 70%, ethanol fraction from the mouse liver, lung, kidney and brain tissues, in the 80% ethanol fraction from the mouse liver and lung tissues; figure of comparison of the MALDI TOF MS protein profiles. This material is available free of charge via the Internet at http://pubs.acs.org.

spatial and anatomic relationships permitting the complex interaction of cells and their environment to be studied at the molecular level.[1–9] From the systematic analysis of a single tissue section, protein-specific maps directly correlated with tissue architecture may be simultaneously obtained for hundreds of different protein species.[1] The potential for this type of analysis in which the spatial distribution of specific molecular species can be mapped throughout a tissue section is particularly exciting for the study of disease.[10–13] While this capability is routinely available for known individual proteins via immunohistochemistry, IMS offers the potential for the simultaneous analysis of many molecular species present in a single biopsy regardless of the availability of specific antibodies. In addition, this technology also permits imaging tissue distribution of low molecular weight compounds such as lipids,[14–18] drugs and metabolites,[19–25] opening new possibilities for the measurement of concomitant protein changes in specific tissues after systemic drug administration.[26] In combination with rapid advances in sample preparation,[9,27–32] and data processing,[33,34] IMS offers the capacity for an entirely new and highly precise means of analyzing tissues.

For the most part, sections from fresh-frozen tissue blocks have been utilized for the direct MALDI IMS analyses of intact proteins. In this case, no fixative agents are added, and when frozen immediately after sampling to minimize protein degradation, the protein profiles and images recovered from the sections should reflect the original proteomic content.[35] Although ideal to work with from a mass spectrometry point of view, fresh-frozen tissues have several drawbacks. First, transport and long-term storage have to be performed at −80 °C or colder. Second, pathologists prefer to make their diagnostic evaluations on sections from fixed tissues, which present more key features than those traditionally observed from fresh-frozen sections. In this respect, sections from formaldehyde (formalin)-fixed tissues are usually preferred. Some MS and IMS-based proteomic studies have been reported from formalin-fixed, paraffin-embedded (FFPE) samples;[36,37] however, such fixed tissues present an enormous challenge from a molecular perspective. Although some of the cross-linking products in tissues have been studied,[38] these generally remain poorly understood. Further, these cross-links are not easily reversible, a step absolutely critical for subsequent whole protein MS analyses. Solvent-only preserved tissues present some advantages: (1) long-term preservation of tissues at room temperature after paraffin embeding, (2) generation of high quality histological sections[39,40] and (3) no chemical alteration of the proteins. Several examples exist in the literature demonstrating the potential of ethanol-fixed tissues for proteomic analyses.[39,41] On the basis of these initial studies, the National Cancer Institute currently recommends fixation using 70% ethanol as standard long-term tissue preservation protocol for further genomic and proteomic studies.[42]

We explore here the use of ethanol-preserved, paraffin-embedded (EPPE) tissue specimens for proteomic analyses by MALDI imaging mass spectrometry. In parallel to the mass spectrometric analyses, histological comparisons between fresh-frozen, formalin-fixed and ethanol-preserved tissue sections are presented. With the use of several control mouse organs, the systematic investigation of several key steps involved in tissue preservation have also been performed, more specifically protein leakage or loss from the tissue specimens during the various dehydration steps. Systematic comparisons of the signals detected from fresh-frozen and ethanol-preserved mouse control organs by MALDI IMS have also been performed. Finally, images from control brain tissue and a tumor bearing mouse lung biopsy were acquired.

Materials and Methods

1. Tissue Specimen Collection and Processing

Mouse lung, kidney, brain and liver tissue samples were either snap-frozen, preserved by progressive alcohol dehydration or fixed by 10% neutral buffered formaldehyde prior to alcohol dehydration. For normal tissue collection, a total of seven animals were used (mature C57BL/6, 8-weeks of age and 25 g). After sacrifices by CO_2 asphyxiation and dissection, the organs from three mice were alcohol-preserved, from two mice were fresh-frozen, and from two mice were formalin-fixed and paraffin-embedded. All preservation processes were initiated immediately after animal sacrifice as rapidly as the tissue specimens could be dissected.

2. Chemicals

Xylene, HPLC grade ethanol (EtOH), 10% neutral formaldehyde (formalin) in PBS, formic acid, acetonitrile, iodocetamide, Tris base (Tris-HCl), dithiothreitol (DTT), and MALDI matrices (sinapinic acid, SA; α-cyano-4-hydroxycinnamic acid, CHCA; and ferrulic acid, FA) were purchased from Sigma Chemical Co. (St Louis, MO). The MALDI matrices were used without further purification. Tris(2-carboxyethyl) phosphine hydrochloride (TCEP) was purchased from Pierce (Rockford, IL). Gel electrophoresis reagents (NuPAGE reducing agent, and NOVEX stainer A and B solutions) were purchased from Invitrogen (Carlsbad CA).

3. Fresh-Frozen Tissue Specimens

After dissection, lungs were inflated with 1 mL of a mixture of 50/50 OCT tissue embedding media/PBS instilled through the trachea which was then ligated and the total lung block snap-frozen in liquid nitrogen. Other tissue specimens were loosely wrapped in aluminum foil and slowly immersed in liquid nitrogen. The frozen samples were then stored in a −80 °C freezer until processed. Thin 8 μm sections (10 μm for lung) were cut at −15 °C using a cryostat (CM 3050 S, Leica Microsystems GmbH, Wetzlar, Germany). The sections were gently deposited on either MALDI compatible metallized (indium–tin oxide coated) glass slides (Delta Technologies Ltd., Stillwater, MN) for MS analyses[28] or standard microscope slides for subsequent staining and histological evaluation and thaw-mounted while inside the cryostat by simply warming the slide (on one's hand). While still holding the slide, macroscopic drying of the section (for ~30 s) was allowed before retrieving the slide from the cryostat. The sections were then allowed to further dry in a desiccator for 1 h before matrix deposition. Prior to matrix deposition, the sections were rinsed at room temperature for 30 s in 70 and 95% ethanol solutions and allowed to dry for a few minutes in a desiccator. The full protocol for tissue sectioning and handling has been detailed elsewhere.[9]

4. Ethanol-Preserved Tissue Specimens

After dissection, lungs were inflated by instilling 1 mL of 70% EtOH via the trachea which was then ligated. Preservation of all tissue specimens then proceeded by immediately plunging the tissue in 10-fold (w/v) 70% EtOH overnight at 4 °C (see Table 1 for weights). Samples were further processed through a series of graded ethanols and xylene (80, 90, 95% EtOH for 2 h at 4 °C, respectively, and 100% xylene for 2 h at room temperature). For each organ, for all of the successive ethanol and xylene dehydration steps, the volumes of solution were kept constant. After use, the graded ethanol and xylene solutions were kept at −20 °C for proteomic analyses. After dehydration, the tissue samples were infiltrated (immersion and vacuum infiltration using a Shandon Excelsior Tissue Processor, ThermoFisher Scientific, Waltham, MA), embedded in paraffin at 65 °C and stored at room temperature. Sections 5 μm thick, were cut from all samples using a microtome (HM325A,

Utech Products, Inc. Schenectady, NY), and either mounted on MALDI compatible conductive glass slides for subsequent MS analyses or standard microscope slides for subsequent staining and histological evaluation. Paraffin removal was accomplished by washes in xylene (100%, twice for 10 s) and graded ethanols (100% twice for 10 s, and in 95, 80 and 70% for 10 s). The slides were then allowed to fully dry in an oven for 1 h at 65 °C.

To estimate protein loss due to leakage from biopsies during the preservation process, protein concentration in each of the graded ethanol fractions was compared to whole organ protein levels via Bradford assay and 1D-gel electrophoresis. Graded fractions were first prepared for quantitation by rotovaping to dryness. Solids were reconstituted in 100 mM ammonium bicarbonate buffered at pH 7.2; 10 mL was used to reconstitute the 70% ethanol fractions, whereas 4 mL was used to reconstitute the 80–100% ethanol fractions. Whole organs (fresh-frozen and ethanol-preserved) were weighed and placed into individual vials. Tissue protein extraction reagent (T-PER, Pierce) was added to each tissue in a ratio of 1/20 (w/v). Glass tissue grind pestles were used to mechanically homogenate whole organs. To further lyse cells, homogenates were subjected to an ultrasonic tip for brief bursts of sonication. Whole organ homogenates were then spun down at 6000 rpm using a swinging bucket rotor and the lysate collected.

For the Bradford assay, samples were pipetted into wells on a polystyrene microplate in 5 μL volumes. Coomassie reagent was added to each sample well until the total volume reached 255 μL. The microplate was shaken for 30 s prior to measurement. Absorbance at 595 nm was measured using a SpectraMax M2 (Molecular Devices, Sunnyvale, CA) to determine total protein concentration. Diluted standards of bovine serum albumin (BSA) served as an analytical calibration.

Reconstituted ethanol fractions and tissue lysates were run on 10–20% Novex Tricine electrophoretic gels (Invitrogen, Carlsbad, CA) with 10 1.0 mm wells. Samples were diluted with SDS running buffer (2×) and NuPAGE reducing agent (10×) in a 4.5/4.5/1 (v/v/v) before loading 15 μL into a gel well. Electrophoresis was carried out at a constant voltage of 125 V with a run time of approximately 60 min. Gels were fixed by shaking for 10 min at room temperature in a solution of 40/50/10 water/methanol/acetic acid. The fixing solution was removed and the gels were initially stained for 10 min in a 55/20/20 mL water/methanol/NOVEX stainer A solution with shaking. After 10 min, 5 mL of NOVEX stainer B was added to the existing solution and shaken at room temperature for 12 h. The stainer B solution was then replaced with water and shaken for 6 h with the water solution replenished every 2 h. Gels were scanned for visual interrogation.

For direct MALDI MS analyses (see below), 1 mL from each of the ethanol fractions was dried down and resuspended in 100 μL of sinapinic matrix (20 mg/mL in 50/50 acetonitrile/trifluoroacetic acid 0.1%). One microliter of each fraction was mixed with an equal amount of matrix (SA, prepared at 20 mg/mL in 50/50 acetonitrile/0.1% trifluoroacetic acid) on the target plate and was allowed to dry prior to MS analyses. The fractions were analyzed by MALDI MS using an Autoflex II time-of-flight mass spectrometer (Bruker Daltonics, Billerica MA) equipped with SmartBeam technology.[43]

5. Formaldehyde-Fixed Tissue Specimens

After dissection, lungs were inflated with 1 mL of 10% neutral buffered formaldehyde in PBS (formalin) through the trachea which was then ligated. All the various tissue specimens destined to be formaldehyde-fixed were immediately plunged in 10% formalin for 24 h at room temperature. The exact same protocol established for specimen preservation by

ethanol dehydration was then followed. Sections for the histological analyses were also cut at a thickness of 5 μm.

6. Tissue Section Staining and Observation

Whole intact organ sections from the fresh-frozen, ethanol-preserved and formalin-fixed, paraffin-embedded tissue specimens were subjected to three common histological stains, hematoxylin and eosin (H&E), Gomori's trichrome, or periodic acid-Schiff (PAS). Each stain was conducted following a standardized protocol (AFIP manual[44]) on an automated histological specimen stainer (Sakura Tissue-Tek DRS 2000, Sakura Finetek USA, Inc., Torrance, CA).

For the EtOH-preserved and formalin-fixed tissues which were paraffin-embedded, once the sections were affixed to slide, they were deparaffinized. This was accomplished by sequentially moving the slides through three changes of xylene, for 2 min each, absolute EtOH, and 2 changes of 95% EtOH, followed by a deionized H_2O rinse.

For H&E staining, briefly, slides were immersed in hematoxylin for 10 min and rinsed twice in H_2O. The slides were then acidified by immersion in 1% HCl in 70% EtOH followed by a running H_2O rinse. The slides were then rinsed in 0.25% NH_4 in H_2O followed by 2 rinses with H_2O. The cytoplasm was counter stained by empirically determined immersion in Eosin, approximately 10 s with agitation. The slides were then ready for dehydration and coverslip mounting.

Gormori's trichrome staining was accomplished by placing the slides in Bouin's solution at 56 °C for 1 h. The slides were washed under running water and then immersed in Gormori's chromium hematoxylin for 10 min followed by a running water wash. The slides were immersed in trichrome blue stain for 15–20 min and then placed in 0.5% acetic acid in H_2O for 2 min. After a deionized H_2O rinse, the slides were ready for dehydration and coverslip mounting.

Slides to be stained by PAS were oxidized in periodic acid solution for 5 min and then rinsed in deionized H_2O. Once drained, the slides were placed in Schiff's reagent for 15 min in a covered coplin jar. To develop the desired color, slides were washed under running water for 5–10 min. Nuclei were counterstained with hematoxylin for <1 min. The slides were then rinsed in deionized H_2O and readied for dehydration and mounting.

Stained slides were dehydrated sequentially through 95% and 100% EtOH and finally xylene, 3 changes each and then coverslips were applied with Permount. Section morphological analyses were performed after scanning the slides using a Mirax Desk microscope slide scanner (Zeiss, Thornwood, NY) at a pixel resolution of 0.23 μm. Digital photomicrographs were exported using the Mirax Viewer software. The prepared samples were assessed in a blinded fashion for staining, architecture, and histological appearance by an experienced pathologist (V.V.P.).

7. Generation of Tumors by Lewis Lung Carcinoma (LLC) Cells

The exact protocol has been detailed elsewhere.[45] Briefly, LLC cells (CRL-1642, ATCC, Manassas, VA) cultured in DMEM supplemented with 10% fetal bovine serum, 4 mM L-glutamine, 1.5 g/L $NaHCO_3$, and 4.5 g/L glucose were administered to mice by inter pleural injection. To induce metastatic lesions, about 1.5×10^5 cells were administered and lung tumors were allowed to develop for 14 days postinjection. After 14 days, the animals were sacrificed by CO_2 asphyxiation. The lungs were inflated and submerged in 70% ethanol (approximately 10× volumes of the lungs) at 4 °C overnight to start the preservation process.

8. Protein Identification from Graded Ethanol Fractions by LC-MS/MS

In-solution protein digestions were performed with mass spectrometry grade trypsin (Trypsin Gold, Promega Corporation, Madison, WI). From the 70% and 80% lung and liver fractions and from 70% brain and kidney fraction, a volume corresponding to an equivalent of 3 μg of total protein was digested. (1) The fractions were evaporated to dryness under a stream of nitrogen and resuspended in 100 μL of a denaturant 6 M urea/100 mM Tris solution. (2) A total of 3 μL of a 200 mM DTT/100 mM Tris reducing agent solution was then added to each fraction. (3) The fractions were incubated for 1 h in the dark at room temperature. (4) A total of 3 μL of a 200 mM iodocetamide/100 mM Tris alkylating reagent was then added to each fraction. (5) The fractions were then incubated for 1 h at room temperature. (6) To capture excess iodocetamide, 3 μL of a 45 mM/100 mM Tris TCEP reducing agent solution was added to each fraction and incubated for 1 h. (7) Prior to enzymatic digestion, 775 μL of milli-Q water was added to each fraction. (8) A total of 1 μL of trypsin solution (200 ng/μL in 100 mM Tris) was added to each fraction and incubated for 3 h at 37 °C. (9) An extra 1 μL of trypsin solution was added and the fractions were incubated overnight at 37 °C. (10) The pH of each fraction was adjusted by adding 50 μL of formic acid. (11) The fractions were desalted using a peptide CapTrap column (model TR1/25109/32, Michrom Bioresources, Inc., Auburn, CA), eluted with 75% acetonitrile and brought down to dryness in a speed vacuum system. (12) The fractions were resuspended in 20 μL of 0.1% formic acid and stored at 4 °C until analyzed by LC-MS/MS.

LC-MS/MS analysis of the resulting peptides was performed using a LTQ linear ion trap mass spectrometer equipped with a MicroAS autosampler and Surveyor HPLC pump, Nanospray source, and Xcalibur 1.4 instrument control (ThermoFinnigan, San Jose, CA). The peptides fractions were diluted by a factor of 10 in 0.1% formic acid prior to separation on a packed capillary tip, 100 μm × 11 cm, with C_{18} resin (Jupiter C_{18}, 5 μm, 300 Å, Phenomonex, Torrance, CA) using an in-line solid phase extraction column that was 100 μm × 6 cm packed with the same C_{18} resin (using a frit generated from liquid silicate Kasil 1,[46] similar to that previously described,[47] except the flow from the HPLC pump was split prior to the injection valve. The flow rate during the solid phase extraction phase of the gradient was 1 μL/min and during the separation phase was 700 nL/min. Mobile phase A was 0.1% formic acid; mobile phase B was acetonitrile with 0.1% formic acid. A 95 min gradient was performed with a 15 min washing period (100% A for the first 10 min followed by a gradient to 98% A at 15 min) to allow for solid phase extraction and removal of any residual salts. After the initial washing period, a 60 min gradient was performed where the first 35 min was a slow, linear gradient from 98% to 75% A, followed by a faster gradient to 10% A at 65 min and an isocratic phase of 10% A at 75 min. MS/MS scans were acquired using an isolation width of 2 amu, an activation time of 30 ms, and activation *Q* of 0.250 and 30% normalized collision energy using 1 microscan and maximum injection time of 100 ms for each scan. The mass spectrometer was tuned prior to analysis using the synthetic peptide TpepK (AVAGKA-GAR). Typical tune parameters were as follows: spray voltage of 1.8 kV, a capillary temperature of 150 °C, a capillary voltage of 50 V and tube lens 100 V. The MS/MS spectra of the peptides were acquired using data-dependent scanning in which one full MS spectrum, using a full mass range of 400–2000 amu, was followed by three MS/MS spectra.

Searches for protein identifications were all carried out as follows using species-specific subsets of the UniRef database: All tandem mass spectrometry data were converted to mzXML format using instrument-specific converting software packages[48] (Institute for Systems Biology, Seattle, WA and Fred Hutchinson Cancer Center) and run through SEQUEST, X!TAN-DEM, and MASCOT separately. X!TANDEM was downloaded from The Global Proteome Machine Organization,[49] while licenses were purchased for the other two search engines (ThermoFisher for SEQUEST, and Matrix Science, Inc., Boston, MA,

for MASCOT). All three of these top matching algorithms were utilized in order to increase confidence in protein identifications, while also decreasing the propensity for false negatives. An example of specifics for each matching program include (1) SEQUEST which is the only algorithm that takes in to account relative, and absolute intensity values generated from each peptide, (2) X!TANDEM, which takes into account partial digests with a focus on B and Y fragment ions, and (3) MASCOT, which takes into account the database size when calculating a unique match. These data are then "combined" and analyzed using protein Prophet (also from the Institute for Systems Biology), which is capable of utilizing all of these data from each output to determine a "best fit" for a specific peptide fragmentation pattern as it relates to an appropriate match from a large database with high confidence. Cutoff filters for protein Prophet vary depending on a dynamically generated probability score that is determined based on each data set. In addition, this approach calculates a true positive correlation as opposed to simply a false positive, common to other approaches. This is important since sample characteristics can change from run to run and since Prophet takes into account both true and false-positives, a more accurate probability score can be determined.

9. MALDI Profiling and Imaging Mass Spectrometry

For tissue profiling, matrix was hand deposited on the sections using a manual pipet. All the MALDI matrices were prepared in the same solvent system: 50/50 acetonitrile/0.1% trifluoroacetic acid. SA was prepared at 20 mg/mL, CHCA was prepared at 10 mg/mL, and FA was prepared saturated. The 250 nL drops of matrix solution were deposited and allowed to dry. To deposit the appropriate amount of matrix for successful analyses, local areas from sections were spotted twice (two 250 nL drops) when prepared with SA, spotted four times when prepared with CHCA, and only spotted once when prepared with FE.

Sample coating for imaging MS was achieved by printing arrays of small matrix droplets using a Portrait 630 reagent multispotter (Labcyte, Sunnyvale, CA). SA was prepared at 20 mg/mL in 40/60 acetonitrile/water with 0.2% trifluoroacetic acid. Matrix was printed with a center-to-center distance of 150 μm by interlacing four print patterns themselves separated by 300 μm center-to-center spacing. Each print pattern was repeated for 15 cycles ejecting 1 drop of matrix per cycle. The volume for each drop was estimated to be ~170 pL. Upon completion, the dimensions of the individual matrix spots achieved were approximately 125 μm in diameter.

All the sections were analyzed by MALDI-TOF MS using an Autoflex II mass spectrometer (Bruker Daltonics, Billerica, MA) operated in the positive linear mode geometry under delayed extraction conditions time focused at ~m/z 15 000. In this case, best resolutions ($M/\Delta M$ measured at full width at half-maximum) close to ~1000 were attainable for ions at or around m/z 15 000, whereas acceptable resolutions in the range of 600 were obtainable for m/z values in the range of 5000 as well as 25 000. IMS data were acquired, assembled and visualized using FlexImaging 2.0 software (Bruker Daltonics, Billerica MA). One mass spectrum was acquired per matrix spot. Each spot was analyzed in the same manner by averaging signals from 250 laser shots acquired in 5 series of 50 shots with each series being acquired on a different location on a spiral pattern within the spot. The collected mass spectra were baseline corrected and intensity normalized by total ion current.[34]

Results and Discussion

1. Histologic Evaluation of Tissue Sections Obtained from Ethanol-Preserved Specimens

To assess the potential of EPPE tissue specimens for histologic evaluations, mouse lung and liver tissues were either ethanol-preserved, formalin-fixed or fresh-frozen. These tissues

present radically different morphologies and densities. Lung tissue is a very diffuse, loosely arranged tissue with elasticity and a complex cellular composition (~40 different cell types), whereas liver tissue is moderately dense, well-organized, cellularly simple (<10 different cell types) and metabolically susceptible to rapid degradation if not properly fixed. Sections from all of the tissue specimens were cut and stained using dyes with different specificities: hematoxylin and eosin (H&E), periodic acid-Schiff (PAS), or Gomori's trichrome. H&E stains the nuclear (purple) and cytoplasmic (pink) content of cells, respectively; PAS primarily stains carbohydrates including mucins; and Gomori's trichrome primarily stains collagens in connective tissues. Microscopic evaluation of stained lung and liver slides was carried out in a blinded manner by a trained pathologist (V.V.P.). All samples were judged well-preserved and adequate for evaluation (Figures 1 and 2).

All samples from the lung (Figure 1) were evenly preserved. This is likely due to the instillation of fixative through the trachea (see Materials and Methods). Also the FFPE (Figure 1A,B,G,H,M,N) and EPPE lung samples (Figure 1C,D,I,J,O,P) showed well-maintained histological structures. As expected, the fresh-frozen specimens (Figure 1E,F,K,L,R,S) exhibited more structural damage (arrows marking septal fragmentation in Figure 1E,L,S) and increased septal thickness (Figure 1, compare arrowheads in panels F versus B, L versus H, and S versus N). This increase in septal thickness limits the fine structure that can be visualized, including individual collagen fibers (Figure 1S versus N).

The formalin-fixed and frozen liver slides showed consistent morphological preservation across the entirety of the tissue section (Figure 2A–F, M–O). As expected the fine detail in all of the frozen sections was more difficult to interpret. This is consistent with normal and long established pathologic expectations. The expansion of water in the tissue upon freezing is the likely cause of this consistent distortion. Even with these findings, all hepatic tissues were histologically well-preserved and hallmark features were easily observed. The ethanol-preserved liver sections showed a decrease in histologic integrity at the center of the section (Figure 2G versus H, I versus J, K versus L). The loss of histologic features can easily be seen in increased vacuolization (Figure 2 arrows in panels G and I compared to H and J), nuclear staining (Figure 2 arrow heads in panels G versus H, I versus J, K vestus L) and the loss of cell–cell margins (Figure 2G,I, K versus H, J, L, respectively). This may be due to the impeded infiltration caused by the connective tissue capsule that surrounds the liver.

This overall pattern observed in the central EPPE liver sections is similar to autolysis, suggesting a slow or delayed preservation. This decrease in integrity was not seen in the lung sections which had ethanol instilled into the tissue as well as emersion fixation from the external surface (see Materials and Methods). Further, lung tissue is thin with a low density and is therefore very permeable which presumably allows a rapid penetration of the ethanol solution. In the case of liver, this suggests that the density of the tissue, the diffusion rate or dilution of the ethanol might be the reason for its uneven preservation.[39] This however was not seen at the periphery of the EPPE sections, suggesting that the histologic changes were preservation artifact and not tissue-based pathology in presumably normal mice. On the basis of our experiences, we recommend that, for tissues with higher cellular densities when ethanol fixation is desired, that these specimens be trimmed into thinner blocks to allow better penetration.[39]

2. Evaluation of Protein Loss from Ethanol-Preserved Tissue Specimens during the Dehydration Process

To evaluate and better understand the effects of the serial alcohol dehydration steps on the proteome, for each of the tissue types studied, the total soluble protein quantities were measured after extraction from fresh-frozen and matched ethanol-preserved specimens using a colorimetric assay. To evaluate protein leakage or loss from the tissue specimens during

the various dehydration steps, protein quantities in the graded ethanol solutions (70, 80, 90 and 100%) were also measured. The various protein extracts were also investigated by 1D-gel electrophoresis and mass spectrometry (MALDI MS). In a third experiment, the ethanol soluble proteins which leaked from the tissues in the 70 and 80% fractions were identified by liquid chromatography coupled with tandem mass spectrometry (LC-MS/MS).

2.1. Protein Quantitation—The sets of organs were chosen to compare total soluble protein quantities recovered after each preservation technique. For each organ studied, protein quantities are presented in Table 1. Overall, efficacy of protein recovery from the ethanol-preserved samples was found to be between 14 and 35% with respect to the quantities obtained from fresh-frozen tissues. This behavior was previously reported and can be in part explained by protein solubilization in the graded ethanols and migration from the specimens into the preservation solutions.[41] Diffused protein amounts measured from the various ethanol preservation fractions are also reported in Table 1. Overall, it can be seen that only a small percentage of the total soluble proteome between ~2 and 7.5% was found in these fractions. This indicates that protein loss by diffusion during the ethanol preservation steps is minimal and does not account for a significant part of the protein loss observed from the ethanol-preserved tissue specimens. Some proteins may be more susceptible to the preservation process and degrade. Other proteins may precipitate *in situ* in the presence of ethanol and may not resolubilize in the extraction buffer. Finally, although ideal for fresh tissues, our protein extraction procedure may not be optimal for ethanol-preserved specimens.

2.2. MALDI MS and 1D-Gel Electrophoresis—In parallel to the protein quantitation assay, a direct MALDI MS measurement was performed on each fraction. As an example, Figure 3A presents the protein mass spectra acquired from the ethanol fractions recovered after dehydration of mouse brain samples. Very similar results were obtained from liver, kidney and lung tissues. Clear signals were observed for the 70, 80 and 90% ethanol fractions. However, significant drops in signal intensities were observed with increasing ethanol percentages. Very low intensity signals were however still detected from the 100% ethanol fraction. These results tend to indicate that the bulk of protein migration happens early on during the dehydration process in the 70% ethanol fraction but is still ongoing in the higher percentage fractions.

These same protein extracts, as well as the extracts obtained from the fresh-frozen and EPPE tissue specimens, were also investigated by 1D-gel electrophoresis. For example, Figure 3B presents the migration results obtained from the brain samples. A significant drop in total proteins extracted from the fresh-frozen and ethanol-preserved samples can again be seen when comparing the overall staining intensity of the corresponding lanes. Only in the 70% ethanol fractions can distinct protein bands be observed above a MW of 7 kDa. The 80, 90 and 100% ethanol fractions only present a migration pattern consistent with low molecular weight species. These species are presumably protein degradation products migrating out of the tissues during the preservation process. This explanation is consistent with the continuous detection of proteomic material in the 80–100% ethanol fractions using the colorimetric assay (Table 1), and the decreasing detection of intact proteins from these same fractions by MALDI MS (Figure 3A).

2.3. Identification of Ethanol Soluble Proteins—To better understand the nature and histological origin of the proteins that solubilize and migrate from the studied tissue specimens during the dehydration process, the proteomic content of the 70 and 80% (liver and lung only) ethanol fractions was characterized by liquid chromatography coupled with tandem mass spectrometry (LC-MS/MS). For each fraction, the recovered proteins were first digested with trypsin and the resulting peptides were automatically fractionated, mass

analyzed and sequenced. The MS and MS/MS results for each peptide were compared against the known mouse genome and proteome. Reliable protein identification was ascertained by the observation of two or more peptides. Table 2 presents the global results from the identification of proteins in the 70% ethanol fractions from mouse liver, lung, kidney and brain with a probability ≥0.5. For most of the proteins identified, the sequence coverage was found high, in numerous cases over 50%. Complete lists of identified proteins for each organ can be found in Supplemental Tables S1–S5. Interestingly, the total number of migrated proteins identified with high confidence from each organ was not found to be very high, ~100 for lung, kidney and brain and significantly lower with only 58 for liver. This lower number can again be explained by the lower number of cell types comprising the liver. Numerous proteins were found with some commonality across tissues, of these 27 were found common to all tissue types (Supplemental Table S5). Numerous other proteins were also found common across three or two organs (Supplemental Table S5). Overall, the number of proteins observed with some commonality across organs represents ~50% of the total number of protein identified for lung, kidney and liver and up to 78% for liver.

One hypothesis for the observation of common proteins is that these are found in the circulatory system. This is certainly the case for proteins like the alpha and beta hemoglobins as well as serum albumin which were consistently observed across all fractions. No comprehensive list of serum proteins exists for mouse. The results were however compared to the proteins identified in human serum compiled by the Human Protein Organization.[50] Overall, about 40% of the proteins observed with some commonality have been observed in human serum. This percentage is however higher, ~56%, for the proteins found in common across all for organs (Supplemental Table S5). These results seem to indicate that a significant fraction of the proteins identified in the 70% ethanol fractions initially used to dehydrate the various tissue specimens have a serologic origin. This is expected since these proteins can freely equilibrate from the vasculature to the preservative.

From each tissue however, ~49% for lung, kidney and brain and 22% for liver of the proteins identified were found to be unique. Of these, several are known to be tissue-specific. This is certainly the case for PEP-19 and the secretogranins-1, -2 and -5 observed from the brain fraction, for the lung carbonyl reductase and the pulmonary surfactant-associated protein B observed from the lung fraction, or for the fatty acid binding protein and the liver carboxypeptidase observed in the liver fraction. This seems to indicate that it is possible that, during the dehydration process, some proteins are sensitive to ethanol penetration within the tissues and will solubilize and delocalize from their original cellular compartments.

Supplemental Tables S6 and S7 present the detailed results from the identification of proteins in the 80% ethanol fractions from mouse liver and lung respectively. The protein content of the brain and kidney 80% ethanol fractions was not found high enough to generate quality data. From each fraction, new proteins not previously seen in the respective 70% fractions were identified. This is particularly true for the 80% lung ethanol fractions: out of the 75 proteins identified, 24 were new. This again tends to indicate that with increasing ethanol percentages within the sequential dehydration procedure, proteins tend to selectively solubilize and migrate from the tissue specimens.

3. Profiling and Imaging of Proteins from Tissue Sections Obtained from Ethanol-Preserved Specimens

3.1. Protein Profiling—The proteomic content of thin sections cut from ethanol-preserved tissue specimens was investigated by MALDI profiling mass spectrometry. To assess the quality of the spectrometric data and to better understand the effect of the

preservation procedure, profiles and images obtained from the ethanol-preserved samples were compared to those obtained from the fresh-frozen samples. For the ethanol-preserved specimens, after sectioning, paraffin removal and partial re-hydration, MALDI matrix (sinapinic acid) was directly deposited on the tissue sections. The sections from the fresh-frozen matching organs were also cut and spotted with the same matrix solution. After solvent evaporation and matrix crystallization, the samples were analyzed by MALDI-TOF MS using the same instrumental settings. Each sample was analyzed in the same manner by averaging signals from 1000 laser shots from random positions within the matrix spots. Figure 4 presents typical protein profiles obtained from fresh-frozen and ethanol-preserved mouse liver in the mass-to-charge (*m*/*z*) range up to 50 000. Supplemental Figure S1 presents similar results obtained for mouse lung. Several general trends were observed. (i) The overall quality of the spectra in terms of resolution, signal-to-noise and overall signal intensity was consistently found better for fresh-frozen sections. The overall number of signals detected from the fresh-frozen and ethanol-preserved section were however fairly similar. (ii) Interestingly, more intense signals were recovered in the lower mass range (from *m*/*z* 2000 up to ~5000) from the ethanol-preserved sections, whereas stronger signals were observed for the mass range above *m*/*z* 18 000 from fresh-frozen sections. This trend was consistently observed for all of the different types of tissues investigated (not shown). (iii) 60% (lung) to 70% (liver) of the mass signals were common to both the fresh-frozen and ethanol-preserved specimens. Various signals, some of which have significant intensities, were unique to traces from one preservation method. Another benefit noted was that, from the analysis of ethanol-preserved tissues sections, little to no hemoglobin signals were observed. This is in sharp contrast with fresh-frozen sections from which on occasions overwhelming hemoglobin signals can be observed leading to evident ion suppression effects. This was found to be particular true for fresh-frozen lung tissue (Supplemental Figure S1).

In a second experiment, different MALDI matrices were tested to assess their compatibility with ethanol-preserved tissue specimens. Figure 5 presents three protein profiles acquired from serial mouse liver sections using CHCA, FA and SA as MALDI matrix. Similarly, Supplemental Figure S2 presents profiles acquired from serial mouse lung tissue with the same three matrices. Overall, all three matrices gave acceptable mass signals up to or in the case of lung over *m*/*z* 20 000. Strong similarities were observed between SA and FA both in terms of the signals observed and their relative intensities. The CHCA matrix gave an abundance of multiply charged signals, particularly from the most abundant protein species. This is clearly shown for the proteins with molecular weights between 13 000 and 16 000 from which singly charged signals are observed, doubly charged signals are observed between *m*/*z* 6500 and 8000 and even triply charged signals are observed between *m*/*z* 4300 and 5300. This is in sharp contrast with the data acquired with SA and FA from which essentially singly charged ion species were observed. Although CHCA overall gave good mass signals from ethanol-preserved tissue sections, the high abundance of multiply charged signals greatly complicate spectrum interpretation and may impair the detection of underlying weaker mass signals.

3.2. Protein Imaging—To further assess eventual protein migration occurring during the dehydration/preservation process, parallel IMS experiments from fresh-frozen and matching ethanol-preserved brain sections were performed (Figure 6). A mouse brain was dissected and separated longitudinally into its two hemispheres. One hemisphere was immediately frozen while the other was ethanol preserved. Sagittal sections were cut from both samples at approximately the same lateral position from the median plane, ~±0.7 mm. Although good mass signals were observed with FA after manual matrix deposition (Figure 5), SA was in this case preferred because of the inconsistencies observed in FA crystallization behavior when microspotted using the automated picovolume matrix dispensing system. SA, on the

other hand, gave very regular and homogeneous spots over the entire array. Brain sections were printed with a final 150 μm center-to-center pitch. The fresh-frozen section was printed with a 88 × 40 = 3520 spot array, whereas the ethanol-preserved section was printed with a 76 × 42 = 3192 spot array. Figure 6 presents the IMS results for a subset of eight signals observed in common from both sections along with the corresponding histologies. The sections were H&E stained after IMS analysis and matrix removal. Different substructures of the mouse brain such as the cerebellum are clearly visible (Figure 6A). Note that, in the case of the EPPE brain, the posterior structure (containing the medulla) below the cerebellum has folded downward. For all of the protein presented, excellent agreement was observed between the images obtained from the fresh-frozen and the ethanol-preserved sections (Figure 6B–I). Each protein signal was found to localize in the same brain substructures. This was found to be true for all of the protein signals detected in common from both IMS measurements. In some cases, the images obtained from the ethanol-preserved section were actually sharper with better contrast with respect to those obtained from the fresh-frozen sample. In view of these results, no protein delocalization effects were observed in the ethanol-preserved specimen, at least at the 150 μm resolution at which the IMS measurements were made.

In a final experiment that was included to gain some appreciation for these techniques in pathologic specimens, we performed a full scale IMS analysis of ethanol-preserved tumor bearing mouse lungs. Tumors were induced by the peritoneal injection of Lewis lung carcinoma cells. In this case, after an incubation period of 14 days, well-defined tumor nodules (1–2 mm in size) were observed along the outer walls of the lungs and upper respiratory airways.[51,52] This is illustrated in the photomicrograph of the ethanol-preserved lung section presented in Figure 7. The entire surface of the section was analyzed by IMS. The section was printed with SA matrix with a 150 μm center-to-center pitch, generating a 76 × 84 = 6384 spot array. From the IMS analysis of the section, over 80 different ion intensity maps were obtained. Figure 7 presents five different ion density maps from proteins, some with very low intensities, which distinctively localize in different areas of the section. For example, the signal at *m*/*z* 4556 clearly localizes within the upper respiratory pathways, the signal at *m*/*z* 8094 has a strong expression in the heart, the signal at *m*/*z* 10 173 is uniquely expressed in lung tissue, whereas the signal at *m*/*z* 4344 correlates well with the presence of major blood vessels. Of interest in the signal at *m*/*z* 6669 which was found in higher abundance in the tumor nodules developing at the surface and within the lungs.

Concluding Remarks

We demonstrate here the possibility of using alcohol-preserved tissue specimens for imaging mass spectrometry analyses. From ethanol-preserved specimens, very high quality histological sections can be obtained which are of better quality than those obtained from fresh-frozen tissue and largely undistinguishable from sections obtained from FFPE blocks.[39] This aspect is important because in some cases, when analyzing sections from fresh-frozen specimens by IMS, the quality of the serially cut and stained section(s) (typically 8–12 μm thick) is limited and renders the observation of some architectural details very difficult. The possibility of using EPPE tissue specimens may for this reason be more advantageous. The ethanol-based dehydration approach allows long-term preservation of the tissue specimens without any cross-linking of the molecular content. This greatly facilitates the proteomic analysis of such preserved samples even though some protein degradation is thought to occur in the presence of high percentage of ethanol. Of additional concern is the potential for some of the proteins present in the specimens at the moment of resection or dissection to migrate or diffuse as the ethanol solution penetrates the tissue. Our results show that the amounts of proteins recovered in the graded ethanol solutions were in the order of a few percent (~6%) of the total soluble proteome indicating that diffusion

phenomena are limited. Further, these diffused proteins were identified using a liquid chromatography coupled with tandem mass spectrometry approach. Ethanol is presumed to primarily penetrate tissues via existing channels such as blood vessels. Indeed, a large number of the 'leaked' proteins were identified as molecules previously observed in serum. A few identified proteins however have origins which were found specific to the processed tissues. This indicates that indeed some proteins may be susceptible and delocalize as a result of alcohol penetration. For certain proteins, this aspect may be critical for the effective meaningfulness of protein images obtained by immunohistochemistry or IMS.

We have nevertheless been successful in obtaining protein profiles and images directly from tissue sections cut from ethanol-preserved tissue specimens by IMS. When compared to the results obtained from fresh-frozen tissue sections, the number of mass signals detected was found similar with 60–70% of these held in common. Some signals were therefore observed unique to one preservation protocol. This indicates that complementary IMS information can be obtained from tissues that have been conserved frozen and ethanol-preserved. IMS measurements performed on mirrored fresh-frozen and ethanol-preserved control mouse brain sections showed identical localization of proteins indicating that no significant protein migration occurs during the preservation process. From the IMS measurements performed from ethanol-preserved tumor bearing mouse lungs, over 80 meaningful protein images were obtained. Some proteins were clearly localized in lung and heart tissues and the upper respiratory pathways, whereas others were localized within the tumor nodules observed at the periphery of the lungs.

These results demonstrate the utility of mass spectrometry to analyze proteins from ethanol-preserved tissues. Tissue prospectively preserved in ethanol requires little additional handling beyond that commonly required for FFPE and is amenable to standard histological preparation and staining. Additionally, EPPE samples can be sectioned with standard microtomes at thicknesses below those commonly employed with frozen sections. This has the advantage of better histologic assessment, better preservation of cellular structures, as well as potentially more precise MS data. In summary, we conclude that ethanol-preserved tissue specimens are amenable to profiling and imaging mass spectrometry, generating high quality protein profiles and images.

Supplementary Material

Refer to Web version on PubMed Central for supplementary material.

Acknowledgments

The authors acknowledge Timothy Blackwell (M.D.) and Taylor Sherrill (Allergy/Pulmonary & Critical Care Med Division, Vanderbilt University) for supplying the mouse tissues; Amy Ham (Ph.D.) and Salisha Hill (Mass Spectrometry Research Center, Vanderbilt University) for their help with the LC-MS/MS data acquisition; and Gregory Bowersock (Department of Surgery, Division of Urology, University of Alabama in Birmingham) for his help with the database searches for protein identification. The authors also acknowledge funding from the National Cancer Institute (grants nos. 5R33 CA116123-3 and 5P30 CA068485-10) and the National Institutes of Health (grant no. 5R01 GM058008-09).

References

1. Stoeckli M, Chaurand P, Hallahan DE, Caprioli RM. Imaging mass spectrometry: A new technology for the analysis of protein expression in mammalian tissues. Nat Med 2001;7(4):493–496. [PubMed: 11283679]
2. Chaurand P, Caprioli RM. Direct profiling and imaging of peptides and proteins from mammalian cells and tissue sections by mass spectrometry. Electrophoresis 2002;23(18):3125–3135. [PubMed: 12298084]

3. Chaurand P, Schwartz SA, Caprioli RM. Imaging mass spectrometry: a new tool to investigate the spatial organization of peptides and proteins in mammalian tissue sections. Curr Opin Chem Biol 2002;6(5):676–681. [PubMed: 12413553]
4. Stoeckli M, Staab D, Staufenbiel M, Wiederhold K-H, Signor L. Molecular imaging of amyloid beta peptides in mouse brain sections using mass spectrometry. Anal Biochem 2002;311(1):33–39. [PubMed: 12441150]
5. Chaurand P, Fouchecourt S, DaGue BB, Xu BJ, Reyzer ML, Orgebin-Crist MC, Caprioli RM. Profiling and imaging proteins in the mouse epididymis by imaging mass spectrometry. Proteomics 2003;3:2221–2239. [PubMed: 14595821]
6. Chaurand P, Schwartz SA, Caprioli RM. Profiling and imaging proteins in tissue sections by mass spectrometry. Anal Chem 2004;76(5):86A–93A. [PubMed: 14697036]
7. Rohner TC, Staab D, Stoeckli M. MALDI mass spectrometric imaging of biological tissue sections. Mech Ageing Dev 2005;126(1):177–185. [PubMed: 15610777]
8. Chaurand P, Cornett DS, Caprioli RM. Molecular imaging of thin mammalian tissue sections by mass spectrometry. Curr Opin Biotechnol 2006;17(4):431–436. [PubMed: 16781865]
9. Chaurand P, Norris JL, Cornett DS, Mobley JA, Caprioli RM. New developments in profiling and imaging of proteins from tissue sections by MALDI mass spectrometry. J Proteome Res 2006;5(11): 2889–2900. [PubMed: 17081040]
10. Schwartz SA, Weil RJ, Thompson RC, Shyr Y, Moore JH, Toms SA, Johnson MD, Caprioli RM. Proteomic-based prognosis of brain tumor patients using direct-tissue matrix-assisted laser desorption ionization mass spectrometry. Cancer Res 2005;65(17):7674–7681. [PubMed: 16140934]
11. Yanagisawa K, Shyr Y, Xu BJ, Massion PP, Larsen PH, White BC, Roberts JR, Edgerton M, Gonzalez A, Nadaf S, Moore JH, Caprioli RM, Carbone DP. Proteomic patterns of tumour subsets in non-small-cell lung cancer. Lancet 2003;362(9382):433–439. [PubMed: 12927430]
12. Chaurand P, Schwartz SA, Caprioli RM. Assessing protein patterns in disease using imaging mass spectrometry. J Proteome Res 2004;3(2):245–252. [PubMed: 15113100]
13. Chaurand P, Sanders ME, Jensen RA, Caprioli RM. Proteomics in diagnostic pathology: profiling and imaging proteins directly in tissue sections. Am J Pathol 2004;165(4):1057–1068. [PubMed: 15466373]
14. Wang HYJ, Jackson SN, McEuen J, Woods AS. Localization and analyses of small drug molecules in rat brain tissue sections. Anal Chem 2005;77(20):6682–6686. [PubMed: 16223256]
15. Jackson SN, Wang HYJ, Woods AS. In situ structural characterization of phosphatidylcholines in brain tissue using MALDI-MS/MS. J Am Soc Mass Spectrom 2005;16(12):2052–2056. [PubMed: 16253515]
16. Jackson SN, Wang HYJ, Woods AS. Direct profiling of lipid distribution in brain tissue using MALDI-TOFMS. Anal Chem 2005;77(14):4523–4527. [PubMed: 16013869]
17. Garrett TJ, Yost RA. Analysis of intact tissue by intermediate-pressure MALDI on a linear ion trap mass spectrometer. Anal Chem 2006;78(7):2465–2469. [PubMed: 16579637]
18. Hankin JA, Barkley RM, Murphy RC. Sublimation as a method of matrix application for mass spectrometric imaging. J Am Soc Mass Spectrom 2007;18(9):1646–1652. [PubMed: 17659880]
19. Troendle FJ, Reddick CD, Yost RA. Detection of pharmaceutical compounds in tissue by matrix-assisted laser desorption/ionization and laser desorption/chemical ionization tandem mass spectrometry with a quadrupole ion trap. J Am Soc Mass Spectrom 1999;10(12):1315–1321.
20. Reyzer ML, Hsieh Y, Ng K, Korfmacher WA, Caprioli RM. Direct analysis of drug candidates in tissue by matrix-assisted laser desorption/ionization mass spectrometry. J Mass Spectrom 2003;38(10):1081–1092. [PubMed: 14595858]
21. Reyzer ML, Caprioli RM. MALDI mass spectrometry for direct tissue analysis: A new tool for biomarker discovery. J Proteome Res 2005;4(4):1138–1142. [PubMed: 16083264]
22. Rudin M, Rausch M, Stoeckli M. Molecular imaging in drug discovery and development: Potential and limitations of non-nuclear methods. Mol Imaging Biol 2005;7(1):5–13. [PubMed: 15912270]
23. Khatib-Shahidi S, Andersson M, Herman JL, Gillespie TA, Caprioli RM. Direct molecular analysis of whole-body animal tissue sections by imaging MALDI mass spectrometry. Anal Chem 2006;78(18):6448–6456. [PubMed: 16970320]

24. Reyzer ML, Caprioli RM. MALDI-MS-based imaging of small molecules and proteins in tissues. Curr Opin Chem Biol 2007;11(1):29–35. [PubMed: 17185024]
25. Stoeckli M, Staab D, Schweitzer A. Compound and metabolite distribution measured by MALDI mass spectrometric imaging in whole-body tissue sections. Int J Mass Spectrom 2007;260(2–3): 195–202.
26. Reyzer ML, Caldwell RL, Dugger TC, Forbes JT, Ritter CA, Guix M, Arteaga CL, Caprioli RM. Early changes in protein expression detected by mass spectrometry predict tumor response to molecular therapeutics. Cancer Res 2004;64(24):9093–9100. [PubMed: 15604278]
27. Schwartz SA, Reyzer ML, Caprioli RM. Direct tissue analysis using matrix-assisted laser desorption/ionization mass spectrometry: practical aspects of sample preparation. J Mass Spectrom 2003;38:699–708. [PubMed: 12898649]
28. Chaurand P, Schwartz SA, Billheimer D, Xu BJ, Crecelius A, Caprioli RM. Integrating histology and imaging mass spectrometry. Anal Chem 2004;76(4):1145–1155. [PubMed: 14961749]
29. Aerni HR, Cornett DS, Caprioli RM. Automated acoustic matrix deposition for MALDI sample preparation. Anal Chem 2006;78(3):827–834. [PubMed: 16448057]
30. Cornett DS, Mobley JA, Dias EC, Andersson M, Arteaga CL, Sanders ME, Caprioli RM. A novel histology-directed strategy for MALDI-MS tissue profiling that improves throughput and cellular specificity in human breast cancer. Mol Cell Proteomics 2006;5(10):1975–1983. [PubMed: 16849436]
31. Lemaire R, Wisztorski M, Desmons A, Tabet JC, Day R, Salzet M, Fournier I. MALDI-MS direct tissue analysis of proteins: improving signal sensitivity using organic treatments. Anal Chem 2006;78(20):7145–7153. [PubMed: 17037914]
32. Lemaire R, Tabet JC, Ducoroy P, Hendra JB, Salzet M, Fournier I. Solid ionic matrixes for direct tissue analysis and MALDI imaging. Anal Chem 2006;78(3):809–819. [PubMed: 16448055]
33. McCombie G, Staab D, Stoeckli M, Knochenmuss R. Spatial and spectral correlations in MALDI mass spectrometry images by clustering and multivariate analysis. Anal Chem 2005;77(19):6118–6124. [PubMed: 16194068]
34. Norris JL, Cornett DS, Mobley JA, Andersson M, Seeley EH, Chaurand P, Caprioli RM. Processing MALDI mass spectra to improve mass spectral direct tissue analysis. Int J Mass Spectrom 2007;260(2–3):212–221. [PubMed: 17541451]
35. Spruessel A, Steimann G, Jung M, Lee SA, Carr T, Fentz AK, Spangenberg J, Zornig C, Juhl HH, David KA. Tissue ischemia time affects gene and protein expression patterns within minutes following surgical tumor excision. BioTechniques 2004;36(6):1030–1037. [PubMed: 15211754]
36. Hood BL, Darfler MM, Guiel TG, Furusato B, Lucas DA, Ringeisen BR, Sesterhenn IA, Conrads TP, Veenstra TD, Krizman DB. Proteomic analysis of formalin-fixed prostate cancer tissue. Mol Cell Proteomics 2005;4(11):1741–1753. [PubMed: 16091476]
37. Lemaire R, Desmons A, Tabet JC, Day R, Salzet M, Fournier I. Direct analysis and MALDI imaging of formalin-fixed, paraffin-embedded tissue sections. J Proteome Res 2007;6(4):1295–1305. [PubMed: 17291023]
38. Metz B, Kersten GFA, Hoogerhout P, Brugghe HF, Timmermans HAM, de Jong A, Meiring H, ten Hove J, Hennink WE, Crommelin DJA, Jiskoot W. Identification of formaldehyde-induced modifications in proteins - Reactions with model peptides. J Biol Chem 2004;279(8):6235–6243. [PubMed: 14638685]
39. Gillespie JW, Best CJ, Bichsel VE, Cole KA, Greenhut SF, Hewitt SM, Ahram M, Gathright YB, Merino MJ, Strausberg RL, Epstein JI, Hamilton SR, Gannot G, Baibakova GV, Calvert VS, Flaig MJ, Chuaqui RF, Herring JC, Pfeifer J, Petricoin EF, Linehan WM, Duray PH, Bova GS, Emmert-Buck MR. Evaluation of non-formalin tissue fixation for molecular profiling studies. Am J Pathol 2002;160(2):449–457. [PubMed: 11839565]
40. Gillespie JW, Gannot G, Tangrea MA, Ahram M, Best CJ, Bichsel VE, Petricoin EF, Emmert-Buck MR, Chuaqui RF. Molecular profiling of cancer. Toxicol Pathol 2004;32(Suppl 1):67–71. [PubMed: 15209405]
41. Ahram M, Flaig MJ, Gillespie JW, Duray PH, Linehan WM, Ornstein DK, Niu S, Zhao Y, Petricoin EF III, Emmert-Buck MR. Evaluation of ethanol-fixed, paraffin-embedded tissues for proteomic applications. Proteomics 2003;3(4):413–421. [PubMed: 12687609]

42. http://cgap-mf.nih.gov/Protocols/Tissues/TissueProtocols/EthanolFixation.html
43. Holle A, Haase A, Kayser M, Höhndorf J. Optimizing UV laser focus profiles for improved MALDI performance. J Mass Spectrom 2006;41(6):705–716. [PubMed: 16718638]
44. Armed Forces Institute of Pathology. Laboratory Methods in Histotechnology. American Registry of Pathology; Washington, D.C: 1994.
45. Stathopoulos GT, Zhu ZW, Everhart MB, Kalomenidis I, Lawson WE, Bilaceroglu S, Peterson TE, Mitchell D, Yull FE, Light RW, Blackwell TS. Nuclear factor-kappa B affects tumor progression in a mouse model of malignant pleural effusion. Am J Respir Cell Mol Biol 2006;34(2):142–150. [PubMed: 16210694]
46. Cortes HJ, Pfeiffer CD, Richter BE, Stevens TS. Porous ceramic bed supports for fused-silica packed capillary columns used in liquid-chromatography. J High Resolut Chromatogr 1987;10(8): 446–448.
47. Licklider LJ, Thoreen CC, Peng JM, Gygi SP. Automation of nanoscale microcapillary liquid chromatography-tandem mass spectromentry with a vented column. Anal Chem 2002;74(13): 3076–3083. [PubMed: 12141667]
48. ProteinProphet SourceForge Site Home page. http://proteinprophet.sourceforge.net/prot-software.html
49. X! TANDEM project Home page. http://www.thegpm.org/TANDEM
50. Center for Computational Medicine and Biology Home page. http://www.bioinformatics.med.umich.edu/hupo/ppp
51. Bertram JS, Janik P. Establishment of a cloned line of Lewis Lung Carcinoma cells adapted to cell culture. Cancer Lett 1980;11(1):63–73. [PubMed: 7226139]
52. Olsson L, Forchhammer J. Induction of the metastatic phenotype in a mouse tumor model by 5-azacytidine, and characterization of an antigen associated with metastatic activity. Proc Natl Acad Sci USA 1984;81(11):3389–3393. [PubMed: 6203119]

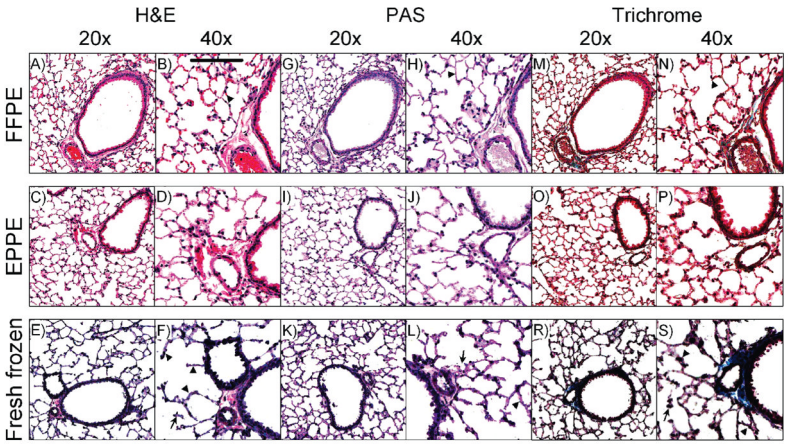

Figure 1.

Histologic comparison of mouse lung tissue sections cut from formalin-fixed, paraffin-embedded (FFPE); ethanol-preserved, paraffin-embedded (EPPE); and fresh-frozen tissue blocks. Sections have been stained with hematoxylin and eosin (H&E), periodic acid-Schiff (PAS), or Gomori's trichrome. Scale bar panel B: 100 μm. See text for details.

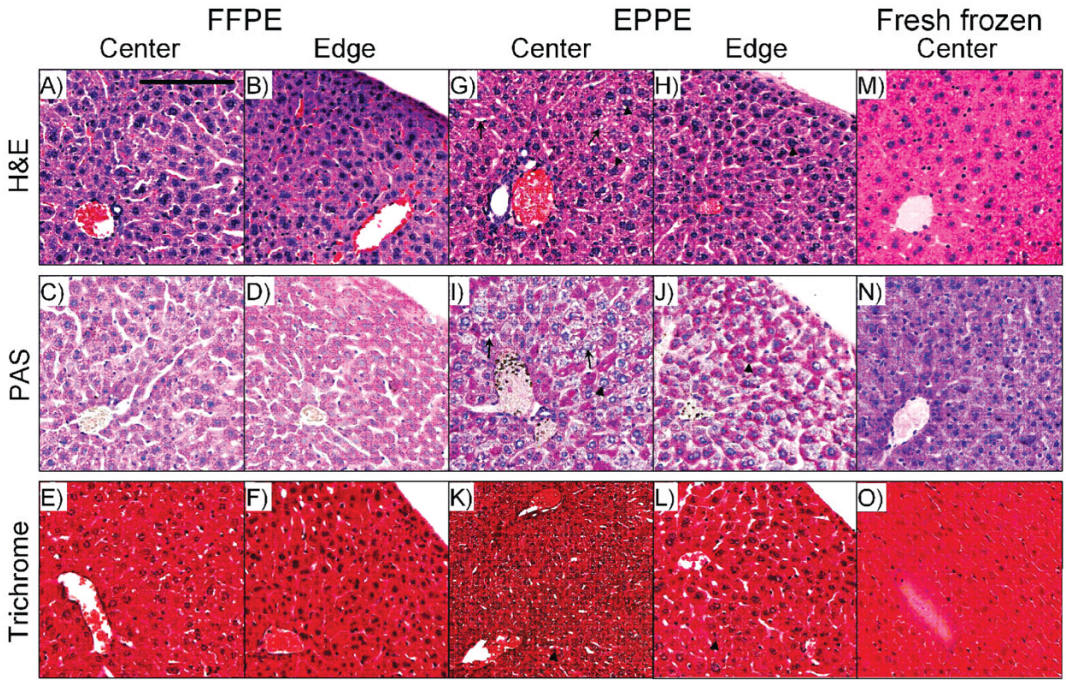

Figure 2.

Histologic comparison of mouse liver tissue sections cut from formalin-fixed, paraffin-embedded (FFPE); ethanol-preserved, paraffin-embedded (EPPE); and fresh-frozen tissue blocks. Sections have been stained with hematoxylin and eosin (H&E), periodic acid-Schiff (PAS), or Gomori's trichrome. Scale bar Panel A: 100 μm. See text for details.

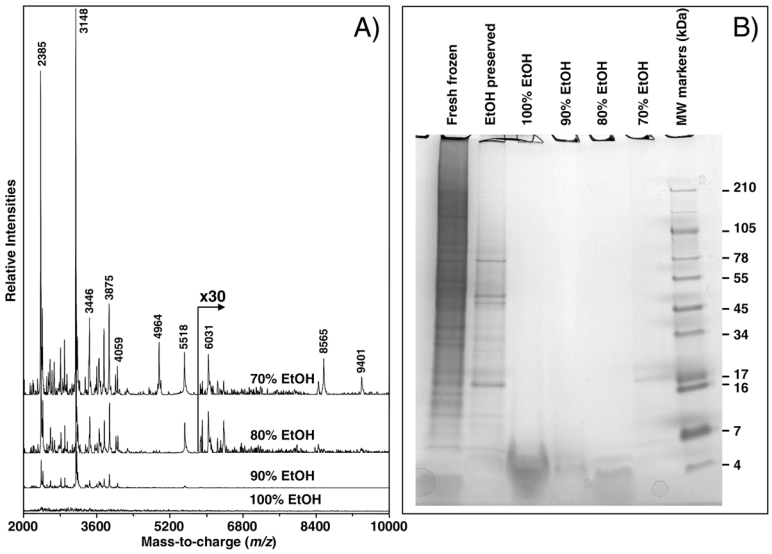

Figure 3.

(A) MALDI-TOF MS protein profiles obtained from graded ethanol fractions used to dehydrate and preserve mouse brain tissue specimens. (B) 1D-gel electrophoresis separation of proteins extracted from fresh-frozen and ethanol-preserved mouse liver as well as for the liver proteins recovered in the 70–100% fractions after the ethanol preservation process.

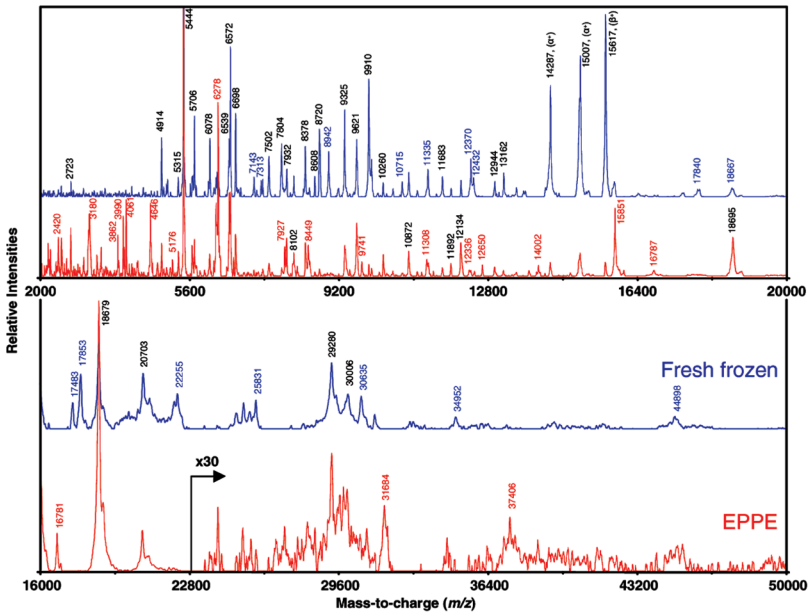

Figure 4.

Comparison of the MALDI-TOF MS protein profiles acquired in the *m*/*z* range from 2000 to 50 000 from fresh-frozen (blue) and ethanol-preserved, paraffin-embedded (EPPE, red) mouse liver tissue sections using sinapinic acid as matrix.

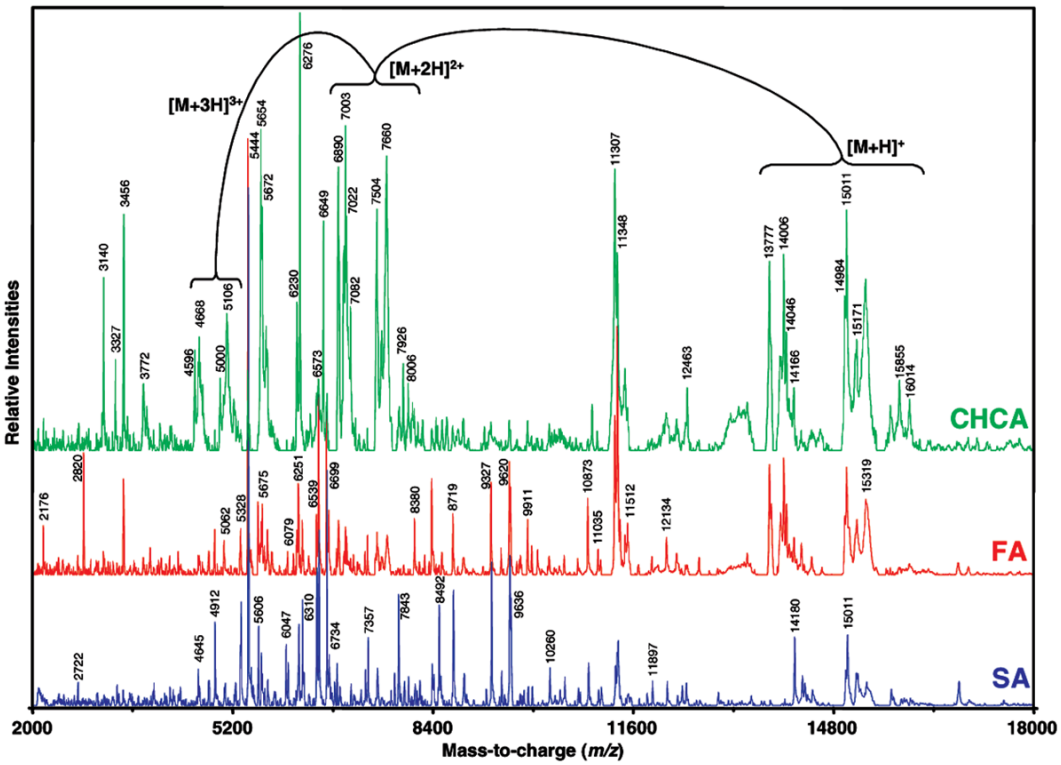

Figure 5.
Comparison of the MALDI-TOF MS protein profiles acquired from ethanol-preserved, paraffin-embedded (EPPE) mouse liver tissue sections using different matrices. SA, sinapinic acid (blue); FA, ferrulic acid (red); CHCA, α-cyano-4-hydroxycinnamic acid (green).

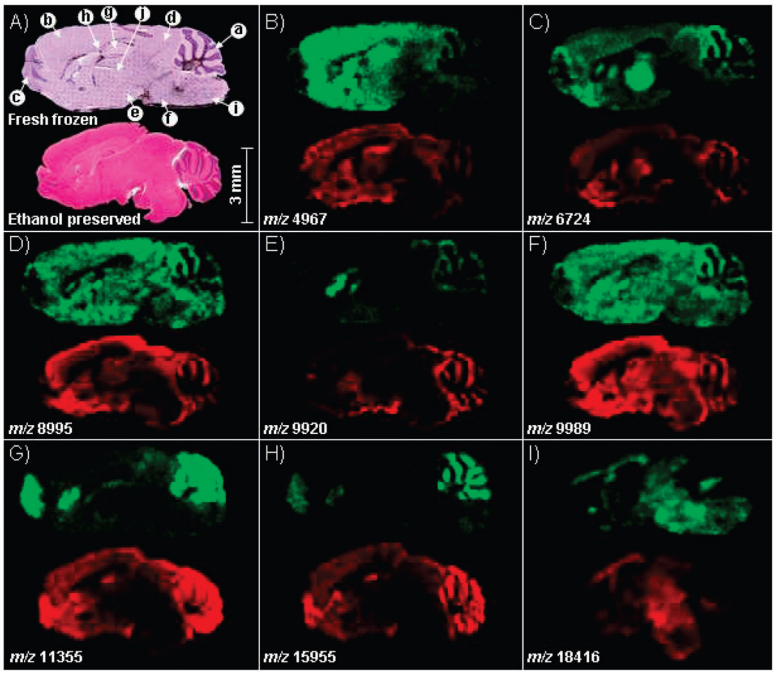

Figure 6.

MALDI IMS analysis of mirrored fresh-frozen and ethanol-preserved sagittal mouse brain sections. (A) Photomicrographs of the sections after H&E staining; (a) cerebellum, (b) cerebral cortex, (c) main olfactory bulb, (d) midbrain, (e) hypothalamus, (f) pons, (g) hippocampal formation, (h) corpus callosum, (i) medulla, (j) thalamus. (B–I) Corresponding ion density maps from a subset of proteins observed in common from both sections. Color intensities correlate with protein abundances.

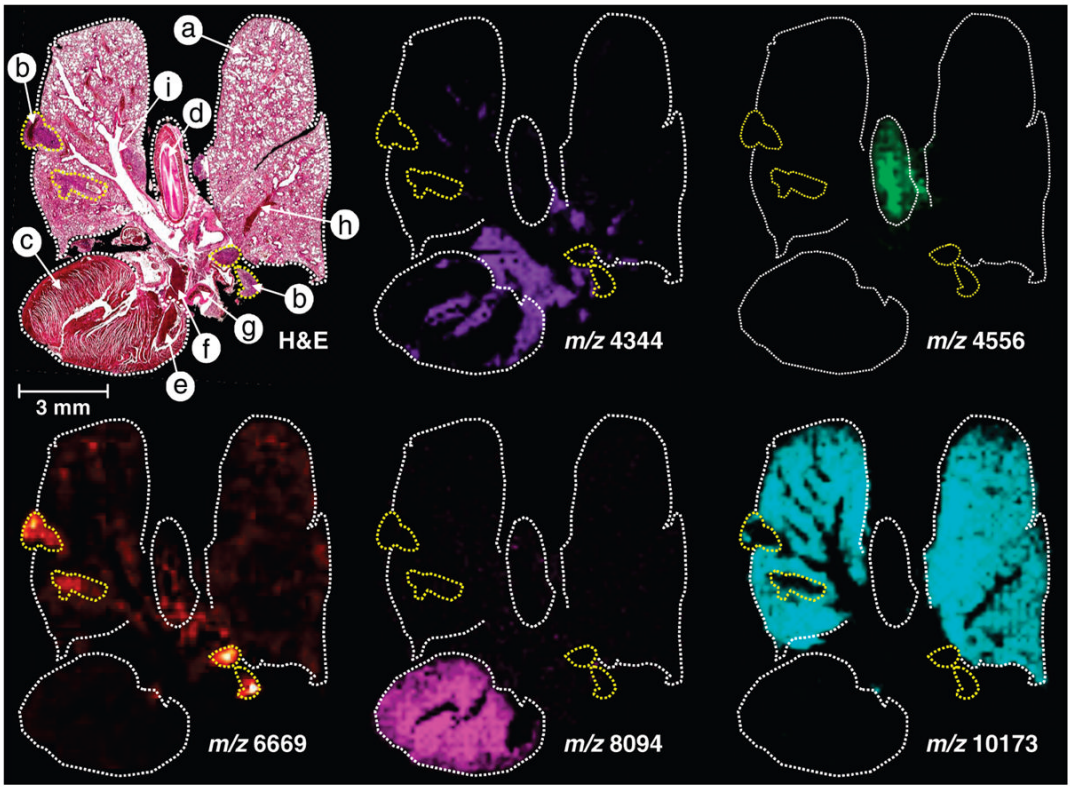

Figure 7.

MALDI IMS analysis of a 5 μm tissue section cut from an EPPE tumor bearing mouse lung specimen. The photomicrograph of the section H&E stained after IMS acquisition and matrix removal presents several different histologies: (a) lung, (b) lung tumors (areas in yellow dotted lines), (c) heart, (d) upper respiratory pathways, (e) left heart ventricle, (f) aorta, (g) right pulmonary artery, (h) artery, (i) bronchus. Five distinct ion density maps from proteins which distinctively localize in different areas of the section are displayed. Color intensities correlate with protein abundances.

J Proteome Res. Author manuscript; available in PMC 2010 August 25.

Table 1

Protein Quantities Measured from Fresh-Frozen and Ethanol-Preserved Mouse Liver, Lung, Kidney and Brain Mouse Tissues as Well as from the 70, 80, 90 and 100% Ethanol Fractions

	total protein per organ (μg) weight of excised organs (mg) ratio (μg/mg)		protein quantity per organ in ethanol fractions total quantity (μg) ratio per mg of excised tissue (μg/mg)					
tissues	**fresh frozen**	**ethanol preserved**	**70%**	**80%**	**90%**	**100%**	**total**	**% leaked**
Liver	82091	18105	290	220	260	321	1091	
	1342	848						
	61.2	21.4	0.34	0.25	0.30	0.37	1.29	**2.1**
Lung	16192	3263	264	137	228	235	864	
	363	294						
	44.6	11.1	0.90	0.46	0.78	0.79	2.94	**6.6**
Kidney	8280	962	133	35	115	229	512	
	189	157						
	43.8	6.1	0.85	0.22	0.73	1.46	3.26	**7.4**
Brain	13660	2131	168	130	213	266	777	
	360	284						
	37.9	7.5	1.07	0.82	1.36	1.69	4.95	**7.2**

Table 2

Global Results from the Identification of Proteins in the 70% Ethanol Fractions from Mouse Liver, Lung, Kidney and Brain[a]

organs	no. of identified proteins ($P \leq 0.5$)	no. of known serum related proteins	no. of common proteins across 2, 3 and 4 organs	no. of unique proteins
Liver	58	23 (40%)	9, 9, 27 (45/58 = 78%)	13 (22%)
Lung	92	34 (37%)	10, 12, 27 (49/92 = 53%)	43 (47%)
Kidney	105	42 (40%)	10, 18, 27 (55/104 = 52%)	50 (48%)
Brain	98	32 (33%)	11, 10, 27 (48/98 = 49%)	50 (51%)

[a]See Supplemental Tables 1–5 for details.